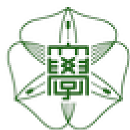

HOKKAIDO UNIVERSITY

Title	Improvements of electronic and optical characteristics of n-GaN-based structures by photoelectrochemical oxidation in glycol solution
Author(s)	Shiozaki, Nanako; Hashizume, Tamotsu
Citation	Journal of Applied Physics, 105(6), 064912 https://doi.org/10.1063/1.3079502
Issue Date	2009-03-15
Doc URL	http://hdl.handle.net/2115/38102
Rights	Copyright 2009 American Institute of Physics. This article may be downloaded for personal use only. Any other use requires prior permission of the author and the American Institute of Physics.
Type	article
File Information	JApplPhys_105_064912.pdf

Instructions for use

Hokkaido University Collection of Scholarly and Academic Papers : HUSCAP

Improvements of electronic and optical characteristics of *n*-GaN-based structures by photoelectrochemical oxidation in glycol solution

Nanako Shiozaki[a),b)] and Tamotsu Hashizume[c)]
Research Center for Integrated Quantum Electronics (RCIQE) and Graduate School of Information Science and Technology, Hokkaido University, Sapporo 060-8628, Japan

(Received 15 November 2008; accepted 4 January 2009; published online 23 March 2009)

Surface control of *n*-GaN was performed by applying a photoelectrochemical oxidation method in a glycol solution to improve the optical and electronic characteristics. The fundamental properties of the oxidation were investigated. The oxidation, chemical composition, and bonding states were analyzed by x-ray photoelectron spectroscopy and micro-Auger electron spectroscopy, in which confirmed the formation of gallium oxide on the surface. The oxide formation rate was about 8 nm/min under UV illumination of 4 mW/cm^2. After establishing the basic properties for control of *n*-GaN oxidation, the surface control technique was applied to achieve low-damage etching, enhancement of the photoluminescence intensity, and selective passivation of the air-exposed sidewalls in an AlGaN/GaN high electron mobility transistor wire structure. The capacitance-voltage measurement revealed the minimum interface-state density between GaN and anodic oxide to be about 5×10^{11} $cm^{-2}\,eV^{-1}$, which is rather low value for compound semiconductors. © *2009 American Institute of Physics*. [DOI: 10.1063/1.3079502]

I. INTRODUCTION

Although recent progress in nitride-based high-frequency and high-power electronics has led to new research fields and applications, serious problems such as current collapse,[1,2] gate leakage current,[3,4] and degradation of light emitting efficiency[5] have limited device performance. These problems are mainly caused by natively existing surface or interface states, and by damage induced during fabrication processes. Therefore, solving these problems requires low-damage processing techniques and suitable passivation methods.[6,7]

Usually, fabrication processes for nitrides are carried out in high-energy environments because nitrides typically have high bond energies, such as 8.0 and 11.5 eV/atom for GaN and AlN, respectively. In dry etching, for example, these high energies are usually supplied by accelerated ions or plasma-assisted species. Dry processes, however, use high-energy reactions with plasma or high-temperature conditions and thus tend to generate surface damage and defects (V_N),[8,9] leading to high-density surface states, formation of shallow donor levels,[10,11] and large leakage currents.[9,12] These surface electronic states can capture carriers, causing to unintentional surface charge up, nonradiative recombination, and Fermi-level pinning, thus affecting device characteristics.

In the research described in this paper, we applied a photoelectrochemical (PEC) process to control the surface of *n*-GaN to improve its electronic and optical characteristics. Since an electrolyte-based wet process uses low-energy chemical or PEC reactions, it can be a low-damage process requiring only one-tenth to one-hundredth of the energy used for a dry process, in a simple setup without a vacuum environment. So far, many approaches for wet surface processing of GaN-based materials have been developed, including surface passivation,[13] etching,[14,15] and damage removal.[16] Recently, the use of wet-gallium oxide for gate dielectrics has demonstrated high transconductance and low leakage current.[17,18] Crystalline gallium oxide (β-Ga_2O_3) itself is also an attractive material for sensing various gases and as a transparent conductive oxide.[19–21] For further practical use of wet oxidation and gallium oxide, it is essential to understand fundamental information about such oxidation and oxides. It is unlikely that the same etching properties given in primary reports can necessarily be obtained because of recent improvements in the crystalline quality of GaN epitaxial layers, including decrease in the residual carrier density. From this viewpoint, intentional carrier generation by UV illumination seems suitable for controlling a wet oxidation process. In this paper, we present a comprehensive study of PEC oxidation on an *n*-GaN surface, covering topics ranging from optimization of the oxidation conditions and the fundamental properties of oxidation and oxides, to applications for improving optical and electronic characteristics.

II. EXPERIMENTAL METHOD

Photoenhanced oxidation of *n*-GaN was carried out in a glycol solution consisting of propylene glycol and 3 wt % tartaric acid at a ratio of 2:1,[22] under potentiostatic control at room temperature, as illustrated in Fig. 1(a). The investigated layer was unintentionally doped single-crystalline metal organic vapor phase epitaxy-(MOVPE) GaN, grown on LT-GaN and an α-sapphire substrate. The thickness of the *n*-GaN layer ranged from 1.8 to 4.5 μm, and typical values of the residual carrier density and the mobility were $1\times10^{16}/cm^3$ and 200–300 $cm^2/V\,s$, respectively. For Ohmic contacts, a multilayer of Ti/Al/Ti/Au (20/50/20/100 nm)[23,24] was deposited on both sides of the GaN surface by electron

a)Corresponding author;
b)Electronic mail: shiozaki@rciqe.hokudai.ac.jp.
c)Electronic mail: hashi@rciqe.hokudai.ac.jp.

 © 2009 American Institute of Physics

Downloaded 25 Mar 2009 to 133.87.129.235. Redistribution subject to AIP license or copyright; see http://jap.aip.org/jap/copyright.jsp

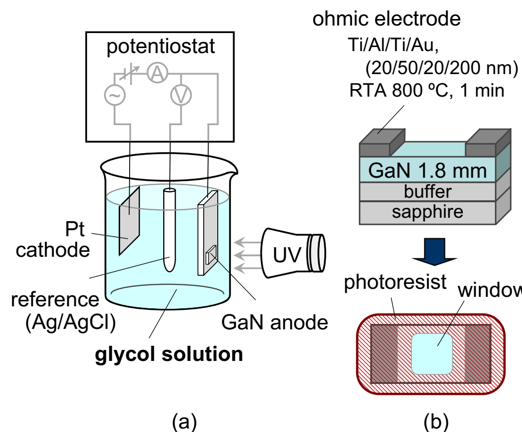

FIG. 1. (Color online) (a) Experimental setup. (b) Sample preparation for oxidation.

beam evaporation, and the sample was subjected to annealing at 800 °C for 1 min in a N_2 ambient. Then, the sample was mounted on a teflon holder with indium metal or silver paste. The oxidation area was defined by photolithography patterning, and the electrodes and edges of the sample were covered with photoresist to prevent current from flowing through these areas, as shown in Fig. 1(b).

Next, the prepared n-GaN sample, a Pt plate, and a Ag/AgCl [E^0(Ag/AgCl)=0.2223 V versus SHE] electrode were connected to a potentiostat, as an anode, cathode, and reference, respectively, and immersed into the glycol solution, whose pH was adjusted to 7.0 by adding NH_4OH. The positively biased GaN sample was oxidized in the glycol solution as follows:[25,26]

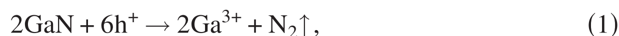

$$2\mathrm{GaN} + 6\mathrm{h}^+ \rightarrow 2\mathrm{Ga}^{3+} + \mathrm{N}_2\uparrow, \quad (1)$$

$$2\mathrm{Ga}^{3+} + 6\mathrm{OH}^- \rightarrow \mathrm{Ga}_2\mathrm{O}_3 + 3\mathrm{H}_2\mathrm{O}, \quad (2)$$

Here, since we used n-type GaN, the GaN surface was exposed to UV light to generate holes, which were essential to the anodic oxidation. The UV light source was a xenon lamp (ASAHI-Spectra, LAX-100), which emitted from 300 to 400 nm and had a power intensity of about 4 mW/cm^2.

The oxidized n-GaN surface was first characterized by x-ray photoelectron spectroscopy (XPS) and micro-Auger electron spectroscopy (μ-AES) measurements, through the use of a Perkin-Elmer PHI 1600, with a monochromatic Al $K\alpha$ source at 1486 eV, and a JEOL Auger Microprobe JAMP-7810, respectively. The photoelectron energy detected by the spectrometer was corrected with gold as a standard sample. The oxide thickness was measured by atomic force microscope (AFM) and ellipsometry. AFM analysis was performed in contact mode with a Digital Instruments Nanoscope III system. The measurement of oxide thickness by AFM was performed with combination of selective etching of the oxide film and step profiling. Photolithographic line-and-space pattern with 4 μm pitch was defined on the oxidized area. Using developer for positive-type photoresist in patterning resulted in etching of gallium oxide for its strong alkaline nature. Thus, height difference between oxide surface and etched GaN surface was measured by AFM as a step profiler. The ellipsometric evaluation of the oxide thickness required a He–Ne laser as a source (ULVAC, Inc.). The AFM measurements also revealed the surface roughness after the oxidation process. Expecting applications for low-damage etching processes and surface passivation for improvements of electronic and optical characteristics, the GaN surface was characterized by XPS after oxide etching. The photoluminescence (PL) properties from the n-GaN's band-edge emission were measured before and after oxidation by using a He–Cd laser (λ=325 nm, Kimmon Co., Ltd.) with a power of 60 mW at room temperature. We also tried selective oxidation of the air-exposed sidewalls of an AlGaN/GaN high electron mobility transistor (HEMT), in order to confirm the electronic passivation effect. Then, passivation effects due to reduction in interface state density for both PL and HEMT wire structure were confirmed by capacitance-voltage (C-V) measurement in metal-oxide-semiconductor (MOS) diode with a use of anodic oxide.

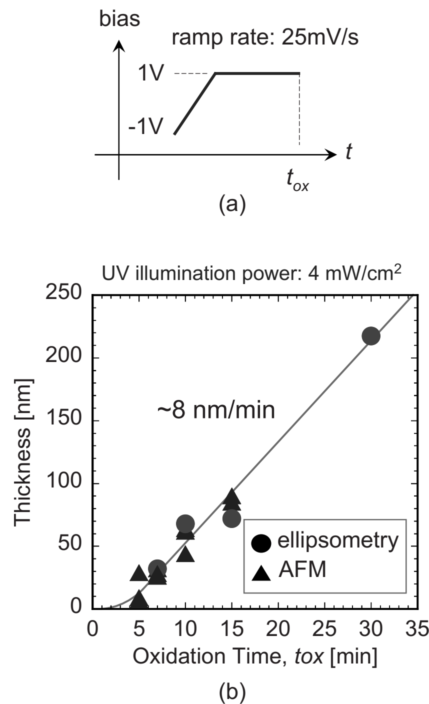

FIG. 2. (a) Bias voltage used for oxidation. (b) Oxide formation rate obtained by ellipsometry and AFM.

III. RESULTS AND DISCUSSION

A. Cyclic voltammetry measurement and oxidation rate

To determine appropriate conditions for oxidation, we first preformed cyclic voltammetry. Obtained I-V characteristics showed the positive current starting to flow from bias voltage of about −1 V, indicating oxidation started from here. Considering that, to maintain surface flatness, the oxidation current should be less than 1 mA/cm^2,[27] the oxidation bias voltage was set to 1 V in this study. We applied a bias whose form consisted of a combination of a ramp from −1 to 1 V at 25 mV/s and a constant bias at 1 V, as shown in Fig. 2(a). This characteristic bias waveform is expected to

Downloaded 25 Mar 2009 to 133.87.129.235. Redistribution subject to AIP license or copyright; see http://jap.aip.org/jap/copyright.jsp

reduce the nonuniform biasing caused by defects at the initial stage of oxidation and to enable gradual formation of uniform oxide on the GaN.

To form oxide films of arbitrary thickness, it is essential to know the oxidation rate. Compared to conventional thermal oxidation or chemical deposition, it is difficult to control the layer thickness formed by wet oxidation because this oxidation reaction has many complex aspects, including a diffusion- or reaction-limited mechanism,[26,28,29] the electrolyte concentration, the pH value, simultaneous dissolution into the electrolyte by, e.g., chelating, and so forth.[30] It is generally understood that the wet oxidation rate is limited by the diffusion of OH^- ions, as with PEC etching of n-GaN.[25,29,31,32] In our oxidation studies, however, we observed current variation with increasing UV light intensity. This indicated that the oxidation rate is mainly limited by the generation of holes. That is, there are a sufficient number of hydroxide ions elsewhere in the electrolyte, and they hardly oxidize the surface when holes are generated there. The fact that the current exhibited almost the same characteristics with and without using a magnet stirrer also supports the assumption that the reaction is not governed only by the diffusion of reaction partners.

From optical measurement by ellipsometry and step measurement by AFM, we found that oxidation under 4 mW/cm^2 of illumination resulted in an oxide formation rate of 8 nm/min, as shown in Fig. 2(b). A typical value of refractive index by ellipsometry was around 1.6–1.8, which were relatively close to common values for Ga_2O_3.[33–35] Note that with a short oxidation time, no oxide was detected by either ellipsometry or AFM. Comparison of the XPS signals for an as-grown GaN surface and one oxidized for 80 s showed almost the same spectra. Typical assumptions for the initial stage of oxidation have been actively discussed for GaAs. Hasegawa *et al.*[22] explained that when the anodic oxide is soluble in the electrolyte, an active-passive transition occurs before surface oxidation. Thus, at the initial stage of the process, oxidation does not occur until the oxidation current exceeds a certain value, j_l. This active-passive transition is well known in the electrochemistry of metals, although the mechanism is unclear. Considering that passivation (i.e., oxidation) of GaAs is more difficult than that of metals, with a much higher j_l,[36,37] the same mechanism might apply to GaN, as well. From the viewpoint of the thermodynamics of oxide film, the energy supplied by the UV illumination could also support dissolution of gallium oxide. Furthermore, it remains possible that part of the initial oxidation current contributes to the generation of oxygen, as follows:

$$2H_2O(l) + 4h^+ \rightarrow O_2(g) + 4H^+, \quad (3)$$

which expresses that the holes generated at the semiconductor surface might oxidize not only the GaN surface, as given by Eqs. (1) and (2), but also water in the electrolyte. The activity at the anode is thus competitive between two reactions.[38] Then, as the oxide layer grows on the surface, the oxidation of water weakens, and uniform oxide formation proceeds.

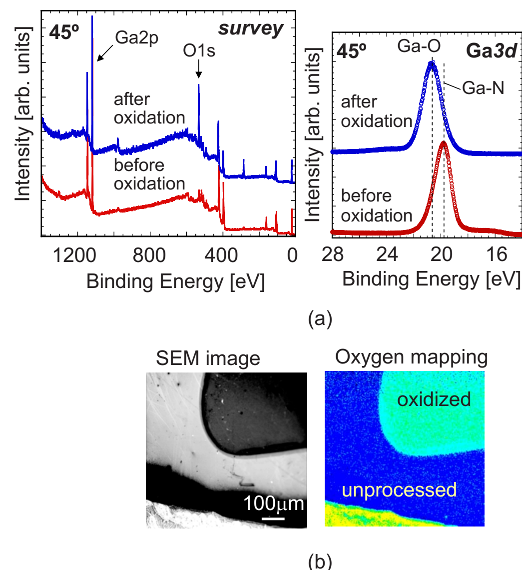

FIG. 3. (Color online) (a) Survey and Ga 3d core-level XPS spectra before and after oxidation for 15 min. (b) SEM and oxygen mapping images of the selectively oxidized n-GaN surface.

B. XPS and μ-AES analyses on processed *n*-GaN surface

The oxidation of the n-GaN surface was confirmed by XPS and μ-AES. Figure 3(a) shows the wide scan and Ga 3d core-level XPS spectra obtained from the surface after 15 min of oxidation, together with those of an as grown, air-exposed n-GaN surface as references. For all measurements, the escape angle was 45°, which corresponds to the signal from a depth of 2–3 nm. The Ga 3d spectrum from the as-grown n-GaN surface had a peak at 19.7 eV, corresponding to the peak due to the Ga–N binding core level. The N 2s peak was also present at around 18 eV, while the O 2s peak was absent.[39–42] On the other hand, a sharp, symmetric peak at 20.8 eV and a broad peak at around 23.5 eV originated from the Ga–O bonding and O 2s core levels after the oxidation process, respectively, indicating that the surface was covered with oxide. The relative intensity ratios of the O 1s and Ga 2p peaks in the survey spectra also reflected the oxidation of the surface. The energy position of Ga–O bonding peak showed that the main composition of the oxidized GaN film was Ga_2O_3. Figure 3(b) shows the elemental peak mapping of oxygen and the corresponding SEM image from the selectively processed n-GaN surface. Oxygen was strongly detected from the oxidized area. Comparison of the differential AES spectra between the unprocessed and oxidized areas showed that the nitrogen peak completely vanished after oxidation, while the elemental mapping for gallium showed a slight difference between the two areas. Thus, the PEC process in the glycol solution oxidized the n-GaN surface, forming gallium oxide.

C. Application to wet etching

The oxidation technique was applied to perform low-damage wet etching, through oxidation of the n-GaN surface and subsequent removal of the oxide. Normally, wet etching consists of oxidation by an electrolyte and subsequent etch-

Downloaded 25 Mar 2009 to 133.87.129.235. Redistribution subject to AIP license or copyright; see http://jap.aip.org/jap/copyright.jsp

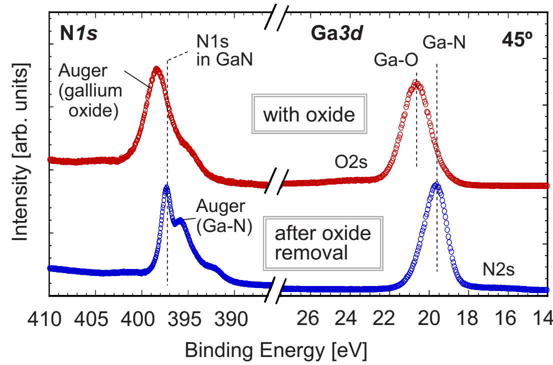

FIG. 4. (Color online) XPS spectra of the N 1*s* and Ga 3*d* core levels before and after etching the oxide layer.

ing of the oxidized area by the same electrolyte. In our experiment, we formed an arbitrary thickness of oxide and then transferred the sample into the etchant. Gallium oxide is soluble in strong acids and alkaline solutions.[43] Here, we used ammonia water and a developer for positive-type photoresist as alkaline solutions. The capability to remove oxide was confirmed by XPS measurements. Upper spectrum shown in Fig. 4 is from a surface with a 100-nm-thick oxide film. After removal of the oxide film by 2 min of etching in the ammonia water, as shown by the lower spectrum in Fig. 4, the N 1*s* characteristic peak emerged at 397 eV instead of the gallium Auger peak at around 395–400 eV. Furthermore, the N 2*s* peak appeared in the Ga 3*d* broad spectrum, indicating that the gallium oxide was clearly removed. Then, the roughness of the GaN surface after oxide removal was investigated by AFM. As a result, the surface with 5 and 10 min of oxidation exhibited root-mean-square (RMS) roughness of 0.7 and 2.1 nm of etched surfaces, respectively. Thus, our wet etching process resulted in low damage etching with smooth surface.

D. Surface passivation effects

Our oxidation technique is promising for surface control because the resulting layer consists of native oxide of the semiconductor, not deposited oxide. Therefore, with a good interface expected between the GaN and oxide, the luminescence was investigated through PL measurement. As shown schematically within the graph of Fig. 5, there was unprocessed as-grown GaN around the oxidized GaN. Thus, two

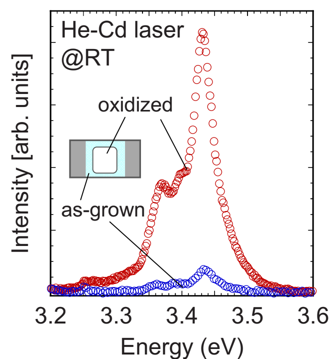

FIG. 5. (Color online) PL spectra from *n*-GaN areas with and without oxide film.

different areas on one chip could be characterized. Figure 5 shows the band-edge emission of the *n*-GaN at room temperature, with and without the oxide film. The spectrum from the oxidized area showed intensities 3–14 times larger than those for the as-grown GaN. This enhancement of the PL intensity could be explained by multiple possible mechanisms, as follows. One is the consumption of the defect-rich layer near the GaN surface into the oxide film. A GaN layer after growth naturally contains many defects near the surface.[3,9,44] These defects tend to generate electronic surface levels that capture carriers, resulting in nonradiative recombination and degradation of the light emitting efficiency. Through oxidation, these defects could have been consumed into the oxide layer: namely, defects near the surface could be reduced by oxidation. Another possible cause is surface passivation effects due to oxidation. The native oxide of the *n*-GaN was expected to form a good interface, resulting in a smooth transition of the bonding configuration, so that dangling bonds were passivated. The passivation of the surface could have relaxed the Fermi-level pinning, consequently leading to reduction of the so-called “dead layer,” the depletion layer. Furthermore, a rougher interface acting as a light-scattering layer or a low refractive index of the oxide could have improved the light extraction efficiency. These factors could all contribute to the enhancement of the PL intensity.

One of the important advantages of wet oxidation is its capability to form a uniform oxide film on any complex structure, as long as the surface is touching the electrolyte. This advantage was demonstrated by selective passivation of a sidewall exposed to air, due to isolation by dry etching, in an AlGaN/GaN HEMT structure. The fabricated HEMT wire structure is shown schematically in Fig. 6(a).We prepared an MOVPE-grown AlGaN/GaN HEMT, which had a 24-nm-thick $Al_{0.27}Ga_{0.73}N$ layer with a mobility of 1380 $cm^2/V\ s$. The Ohmic contacts were formed for source and drain electrodes of HEMT wire device structures. The contact pad with a size of 2×2 mm for anodic oxidation was also formed in the edge of the sample substrate, which was extended from source electrode. Wire structures with a width of 500–800 nm were formed by reactive ion beam etching in a plasma of $CH_4/H_2/Ar/N_2$ [5/15/3/3 SCCM (SCCM denotes cubic centimeter per minute at STP)] to a depth of about 100 nm, by using a SiO_2 mask prepared by EB lithography and wet etching in buffered HF. The SiO_2 at the top of the wire was then reused as a mask for selective oxidation of the air-exposed sidewalls. Without formation of gate electrodes, I_{DS} was measured before the sidewall oxidation. Subsequently, selective oxidation was carried out, with whole surface including source and drain contacts being covered by photoresist except for top and edges of the wires. As the top surface of the wire was already covered with SiO_2, the edges of the wires are only due to be oxidized. The contact pad for anodic oxidation on the substrate was drawn by In wire to the external electrochemical setup, and then protected by photoresist from the electrolyte. The 5 min of oxidation resulted in the formation of about 5 nm of oxide film. Then, I_{DS} was measured again without removing the SiO_2 mask.

Figure 6(b) shows a typical V_{DS}-I_{DS} characteristics of a sample with a wire width of 500 nm before and after selec-

Downloaded 25 Mar 2009 to 133.87.129.235. Redistribution subject to AIP license or copyright; see http://jap.aip.org/jap/copyright.jsp

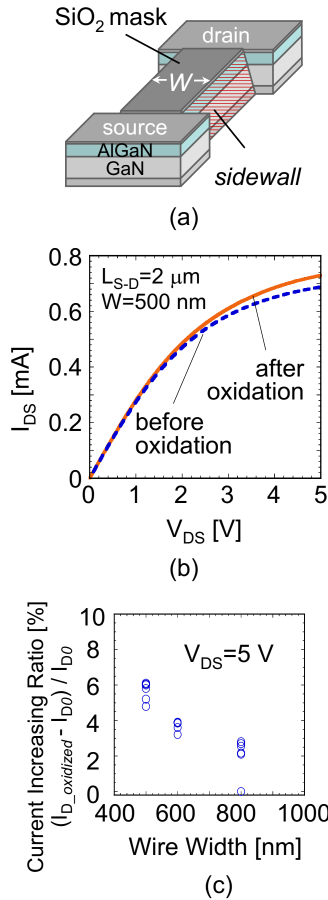

FIG. 6. (Color online) (a) Schematic sample structure of an AlGaN/GaN HEMT wire device with air-exposed sidewalls. (b) I_{DS}-V_{DS} characteristics obtained for an HEMT wire structure with a wire width of 500 nm. (c) Relation between the wire width and current increase ratio.

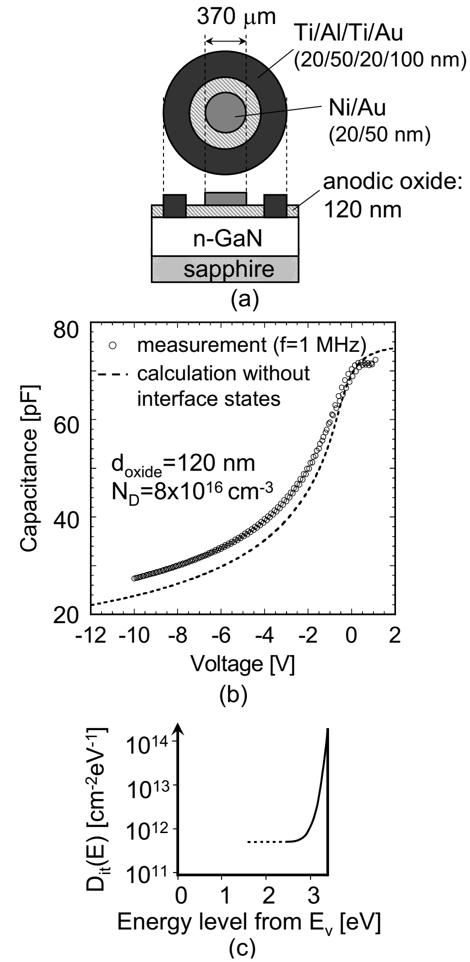

FIG. 7. (a) MOS structure used for C-V measurement. (b) C-V characteristics measured at 1 MHz and calculated. (c) Distribution of interface state density, D_{it}, obtained by Terman method.

tive oxidation. The I_{DS} increased after oxidation, although the wire width was reduced. The dependence of increment of I_{DS} on wire width was investigated using

$$\text{current increasing ratio} = \frac{I_{D_\text{oxidized}} - I_{D0}}{I_{D0}}[\%], \tag{4}$$

where I_{D0} and I_{D_oxidized} indicated the I_{DS} before and after sidewall oxidation, at $V_{DS}=5$ V. It is noteworthy that, as shown in Fig. 6(c), the current increase after oxidation became more pronounced as the channel narrowed, that is, as the proportion of sidewall area accounting for the total surface area increased. Generally speaking, the current must have decreased when the wire width was reduced by oxidation. In our case, however, the dry process for recess etching induced high-density surface states on the sidewall and depleted the channel from both sides, causing geometric reduction of the wire width, as follows:

$$\frac{W_{\text{cond}}}{W_{\text{top}}} = \frac{W_{\text{top}} - 2W_{\text{dead}}}{W_{\text{top}}} = 1 - 2\frac{W_{\text{dead}}}{W_{\text{top}}} \tag{5}$$

Here, the total wire width, W_{top}, is considered to consist of the effective channel width, W_{cond}, which carries the current, and the dead layer width, W_{dead}, which is depleted by the Fermi-level pinning. Then, $W_{\text{cond}}/W_{\text{top}}$ indicates the ratio of effective channel width. Provided W_{dead} is independent of the wire width, its influence becomes more obvious as the wire narrows. Hence, through oxidation, the high-density surface states were passivated and the sidewall depletion was relaxed, causing the current to increase. Thus, our oxidation technique could selectively passivate the electronic surface states.

E. Ga_2O_3/GaN interface characterization by using MOS structure

To confirm that the improvements in both the PL and the I-V characteristics, as shown so far, were due to the passivation effect by oxidation, the density of interface states between the n-GaN and oxide was estimated for a MOS structure. Figure 7(a) shows the sample structure. After formation of the anodic oxide with a thickness of 120 nm, a ring-shaped Ohmic contact was formed on the n-GaN where oxide was selectively etched. Annealing at 800 °C for 1 min in a N_2 ambient was followed by evaporation of a circular Ni/Au gate electrode at the center of the Ohmic ring.

Figure 7(b) shows the C-V curve measured at 1 MHz, together with the calculation result without taking account of interface states. The experimental result was very close to the calculated one. From the capacitance difference between them, the distribution of the interface state density was cal-

Downloaded 25 Mar 2009 to 133.87.129.235. Redistribution subject to AIP license or copyright; see http://jap.aip.org/jap/copyright.jsp

culated using the so-called Terman method. As a result, interface state densities were found to have relatively low values for compound semiconductors, as shown in Fig. 7(c). The minimum density is 5×10^{11} cm^{-2} eV^{-1} at around $E_C - 1.0$ eV. Bae and Lucovsky[45] reported that the SiO_2/GaN interface with oxidation of the GaN surface showed the minimum interface trap density, D_{it_min}, of $\sim 7\times10^{11}$ cm^{-2} eV^{-1}, while one without oxidation exhibited $\sim 4\times10^{12}$ cm^{-2} eV^{-1}. Their oxidation process using the low-temperature remote-plasma assisted technique led to the formation of an ultrathin GaO_x layer on GaN, which seemed to act as an interfacial control layer. Then, supported by their results, it could be concluded the anodically grown native gallium oxide at the present study also effectively terminated dangling bonds at the GaN surface with a smooth atomic configuration. This probably resulted in the passivation of surface states, leading to the enhancement of the PL intensity and the drain current in samples with the surface control process using anodic oxidation.

IV. CONCLUSIONS

We have demonstrated the oxidation of an *n*-GaN surface by PEC oxidation in a glycol solution. The bias-controlled oxidation under 4 mW/cm^2 of UV illumination led to the formation of gallium oxide with a composition close to Ga_2O_3, at an oxidation rate of 8 nm/min. The oxidation rate was considered to be limited mainly by the UV illumination power, which correlated with the density of photogenerated holes. After oxidation, subsequent etching in an alkaline solution completely removed the oxide film. Expecting to observe a passivation effect due to the oxidation, we measured the PL intensity from the *n*-GaN surface with and without oxide film. The PL intensity from oxidized areas was over ten times higher than that from areas with as-grown GaN. The air-exposed sidewalls in an AlGaN/GaN HEMT wire structure were selectively oxidized. We observed an increase in I_{DS} after the oxidation, although the channel width of the HEMT wire was reduced. This effect became more obvious as the wire width narrowed, indicating an electronic passivation effect on the sidewalls. Finally, *C-V* measurement at 1 MHz of a MOS structure with an oxide thickness of 120 nm obtained D_{it_min} of 5×10^{11} cm^{-2} eV^{-1} between the anodic oxide and the *n*-GaN. This result strongly confirmed the passivation effect in improving both the PL intensity and the *I-V* characteristics for the HEMT wire structure.

[1] M. A. Khan, M. S. Shur, Q. C. Chen, and J. N. Kuznia, Electron. Lett. **30**, 2175 (1994).
[2] R. Vetury, N. Q. Zhang, S. Keller, and U. K. Mishra, IEEE Trans. Electron Devices **48**, 560 (2001).
[3] J. Kotani, T. Hashizume, and H. Hasegawa, J. Vac. Sci. Technol. B **22**, 2179 (2004).
[4] T. Hashizume, J. Kotani, and H. Hasegawa, Appl. Phys. Lett. **84**, 4884 (2004).
[5] Y. Li, X. Yi, X. Wang, J. Guo, L. Wang, G. Wang, F. Yang, Y. Zeng, and J. Li, Proc. SPIE **6841**, 68410X–1-6 (2007).
[6] T. Hashizume, S. Ootomo, T. Inagaki, and H. Hasegawa, J. Vac. Sci. Technol. B **21**, 1828 (2003).
[7] G. Pozzovivo, J. Kuzmík, S. Golka, W. Schrenk, G. Strasser, D. Pogany, K. Čičo, M. Ťapajna, K. Fröhlich, J.-F. Carlin, M. Gonschorek, E. Feltin, and N. Grandjean, Appl. Phys. Lett. **91**, 043509 (2007).
[8] T. Hashizume and R. Nakasaki, Appl. Phys. Lett. **80**, 4564 (2002).
[9] T. Hashizume and H. Hasegawa, Appl. Surf. Sci. **234**, 387 (2004).
[10] J. Neugebauer and C. G. Van de Walle, Phys. Rev. B **50**, 8067 (1994).
[11] P. Bogusławski, E. L. Briggs, and J. Bernholc, Phys. Rev. B **51**, 17255 (1995).
[12] J. Kuzmík, P. Javorka, M. Marso, and P. Kordoš, Semicond. Sci. Technol. **17**, L76 (2002).
[13] H.-M. Wu and L.-H. Peng, Phys. Status Solidi C **3**, 2291 (2006).
[14] C. Youtsey, I. Adesida, L. T. Romano, and G. Bulman, Appl. Phys. Lett. **72**, 560 (1998).
[15] T. Rotter, J. Aderhold, D. Mistele, O. Semchinova, J. Stemmer, D. Uffmann, and J. Graul, Mater. Sci. Eng., B **59**, 350 (1999).
[16] J.-M. Lee, K.-S. Lee, and S.-J. Park, J. Vac. Sci. Technol. B **22**, 479 (2004).
[17] D. Mistele, T. Rotter, Z. Bougrioua, K. S. Röver, F. Fedler, H. Klausing, J. Stemmer, O. K. Semichinova, J. Aderhold, and J. Graul, Phys. Status Solidi A **188**, 255 (2001).
[18] L.-H. Huang, S.-H. Yeh, C.-T. Lee, H. Tang, J. Bardwell, and J. B. Webb, IEEE Electron Device Lett. **29**, 284 (2008).
[19] M. Bartic, Y. Toyoda, C. I. Baban, and M. Ogita, Jpn. J. Appl. Phys. Part 1 **45**, 5186 (2006).
[20] M. Passlack, E. F. Schubert, W. S. Hobson, M. Hong, N. Moriya, S. N. G. Chu, K. Konstadinidis, J. P. Mannaerts, M. L. Schnoes, and G. J. Zydzik, J. Appl. Phys. **77**, 686 (1995).
[21] E. G. Víllora, K. Shimamura, Y. Yoshikawa, T. Ujiie, and K. Aoki, Appl. Phys. Lett. **92**, 202120 (2008).
[22] H. Hasegawa and H. L. Hartnagel, J. Electrochem. Soc. **123**, 713 (1976).
[23] D. F. Wang, F. Shiwei, C. Lu, A. Motayed, M. Jah, S. N. Mohammad, K. A. Jones, and L. Salamanca-Riba, J. Appl. Phys. **89**, 6214 (2001).
[24] A. V. Davydov, A. Motayed, W. J. Boettinger, R. S. Gates, Q. Z. Xue, H. C. Lee, and Y. K. Yoo, Phys. Status Solidi C **2**, 2551 (2005).
[25] T. Rotter, D. Mistele, J. Stemmer, F. Fedler, J. Aderhold, J. Graul, V. Schwegler, C. Kirchner, M. Kamp, and M. Heuken, Appl. Phys. Lett. **76**, 3923 (2000).
[26] D. Zhuang and J. H. Edgar, Mater. Sci. Eng., R. **48**, 1 (2005).
[27] M. Ohkubo and O. Takai, IPAP Conf. Ser. **1**, 770 (2000).
[28] C. Youtsey, I. Adesida, and G. Bulman, Appl. Phys. Lett. **71**, 2151 (1997).
[29] M. Hall, M.-F. Rau, and J. W. Evans, J. Electrochem. Soc. **133**, 1934 (1986).
[30] R. M. Finne and D. L. Klein, J. Electrochem. Soc. **114**, 965 (1967).
[31] C. Youtsey, I. Adesida, and G. Bulman, Electron. Lett. **33**, 245 (1997).
[32] H. Cho, S. M. Donovan, C. R. Abernathy, S. J. Pearton, F. Ren, J. Han, and R. Shul, MRS Internet J. Nitride Semicond. Res. **4 S1**, G6.40 (1999); http://nsr.mij.mrs.org/4S1/G6.40/.
[33] *CRC Handbook of Chemistry and Physics 1989–1990* (CRC, Boca Raton, 1989), p. B-92.
[34] W. Klemm and H. U. Vogel, Z. Anorg. Allg. Chem. **219**, 45 (1934).
[35] S. M. Spitzer, B. Schwartz, and M. Kuhn, J. Electrochem. Soc. **120**, 669 (1973).
[36] W. W. Harvey, J. Electrochem. Soc. **114**, 472 (1967).
[37] W. W. Harvey and J. Kruger, Electrochim. Acta **16**, 2017 (1971).
[38] L.-H. Peng, C.-W. Chuang, J.-K. Ho, C.-N. Huang, and C.-Y. Chen, Appl. Phys. Lett. **72**, 939 (1998).
[39] S. D. Wolter, B. P. Luther, D. L. Waltemyer, C. Önneby, S. E. Mohney, and R. J. Molnar, Appl. Phys. Lett. **70**, 2156 (1997).
[40] R. Carin, J. P. Deville, and J. Werckmann, Surf. Interface Anal. **16**, 65 (1990).
[41] J. Hedman and N. Martensson, Phys. Scr. **22**, 176 (1980).
[42] Y. Mizokawa, O. Komoda, and S. Miyase, Thin Solid Films **156**, 127 (1988).
[43] M. Pourbaix, *Atlas of Electrochemical Equilibria in Aqueous Solutions*, 2nd English ed. (National Association of Corrosion Engineers, Houston, 1974).
[44] J. Kotani, M. Kaneko, H. Hasegawa, and T. Hashizume, J. Vac. Sci. Technol. B **24**, 2148 (2006).
[45] C. Bae and G. Lucovsky, J. Vac. Sci. Technol. A **22**, 2402 (2004).

Downloaded 25 Mar 2009 to 133.87.129.235. Redistribution subject to AIP license or copyright; see http://jap.aip.org/jap/copyright.jsp